Progress In Electromagnetics Research B, Vol. 36, 151–171, 2012

ACCURATE REPRESENTATION OF EXCITATION AND LOADING FOR ARBITRARILY SHAPED ANTENNAS COMPOSED OF CONDUCTING SURFACES IN THE METHOD OF MOMENTS

K. F. A. Hussein*

Microwave Department, Electronics Research Institute, Cairo, Egypt

Abstract—In this work, a new method is introduced to model the excitation and loading for antennas composed of arbitrarily shaped conducting surfaces treated by the elctric field integral equation method described by Raw-Wilton-Glisson (RWG). Instead of using a single non-boundary edge to represent a zero-width exciting gap according to the conventional method, the proposed method uses either single or multiple pairs of facing boundary edges to form a real gap of arbitrary shape and width. The new method has many advantages over the conventional (zero-width) source/load representation considering the flexibility in shaping the gap to fit the antenna surface and the accuracy of the obtained results especially for the antenna input impedance and the input current distribution. The new method is described mathematically in detail. Modified basis functions are described for the gap source/load. Numerical results are obtained to investigate the dependence of the antenna input impedance and the current distribution along the gap length on the gap width, the geometrical shape of the gap and the surface segmentation resolution along the gap length.

1. INTRODUCTION

Modeling the feeding sources and loads in three-dimensional problems of multi-port antennas and waveguide sections is one of the most important and critical issues in the computational electromagnetic techniques. For dependable results, such models should accurately represent the actual source or load. This includes the actual geometry, electric properties, voltage and/or current distributions, internal source or load impedance and its actual distribution.

Received 7 October 2011, Accepted 2 November 2011, Scheduled 9 November 2011

* Corresponding author: Khalid Fawzi Ahmed Hussein (Khalid_elgabaly@yahoo.com).

In most antenna problems, the key variables of interest are typically the input impedance at a particular feed location and the resulting radiation pattern, directivity and gain. The easiest way to compute these is to consider the antenna in its transmitting mode, requiring a reasonable model of the feed system at the input terminals. Practically, an antenna is fed by an transmission line or by a coaxial feed through a ground plane. These various feed systems affect the antenna impedance characteristics in different ways. Many types of source models have been applied to the method of moments (MoM). The most commonly used source model is the so-called delta gap source model. The delta-gap source treats the feed as if the electric field impressed by the feed line exists only in the gap between the antenna terminals and is zero outside, i.e., no fringing. This method typically produces less accurate results for input impedance though it still performs very well for computing radiation patterns [1, Chapter 4, p. 65]. According the assumption of this source model, the element of the voltage vector corresponding to the driving segment has unit value and the other elements have values of zero voltage. This model has been used extensively because of its simplicity. However, one of its drawbacks is that the current at the feed segment depends on the length of the divided segments [2].

For arbitrarily-shaped antennas composed of conducting surfaces, the gap voltage source model is appropriate to model the excitation in the MoM. In [3], Raw-Wilton-Glisson (RWG) basis functions are defined to expand the unknown current distribution on the conducting surface. In [4, Chapter 4, p. 61, 65] and [5], the gap source is represented by a non-boundary edge across which a voltage drop equal to the exciting voltage is enforced. This is implemented by setting the corresponding element of the V vector in the MoM equation, $ZI = V$, to the value of the applied voltage divided by the length of the non-boundary edge representing the gap source. In this model, the excitation gap width is assumed zero (or infinitesimal), which may not be the actual case. Using the method of [4, Chapter 4, p. 61, 65] and [5], there is no way to represent an excitation gap with a non-zero width. This actually affects the accuracy of the evaluated input impedance, which is strongly dependent on the exciting source representation.

It may be worthwhile to mention that more accurate and realistic models are described to represent the source in the method of moments in [6, 7].

2. NONZERO-WIDTH GAP SOURCE REPRESENTATION

In the EFIE technique described in [3], the conducting surface is modeled using a number of N connected triangular patches as shown in Figure 1(a). Each triangular patch has three edges. Any two adjacent triangular patches share an edge, which is referred to as a *nonboundary* edge. An edge that belongs to only one triangular patch is referred to as a *boundary* edge and lies on the conducting surface rim.

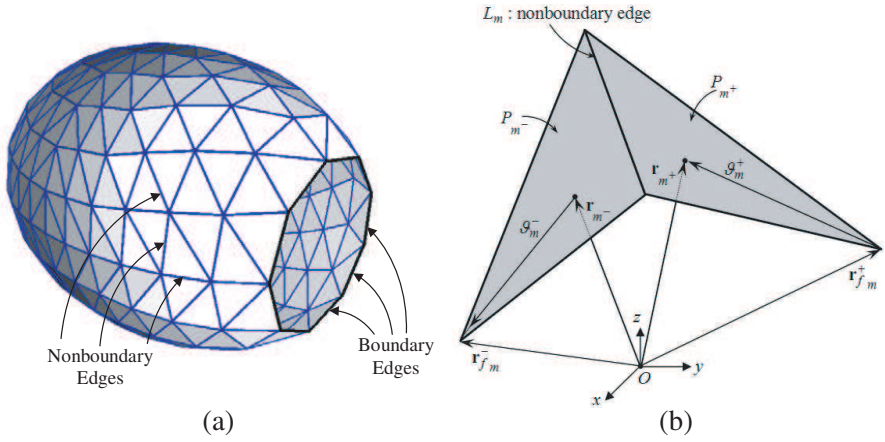

Figure 1. (a) Triangular-patch model of a conducting surface. (b) Two adjacent triangular patches.

For a computational model of the conducting surface, the triangular patches and the nonboundary edges are indexed as shown in Figure 1(b). An unknown linear current density is assumed perpendicularly crossing each of the nonboundary edges. This current density is assumed constant over the nonboundary edge. The distribution of the linear current density on the conducting surface is expressed as

$$K = \sum_{m=1}^{N} K_m f_m \tag{1}$$

where N is the number of the nonboundary edges of the surface model, K_m is the unknown linear current density crossing the mth nonboundary edge and f_m is the RWG basis function defined over the

areas of P_{m^+} and P_{m^-} as

$$\mathbf{f}_m(\mathbf{r}) = \begin{cases} \dfrac{l_m}{2S_{m^+}}\vartheta_m^+(\mathbf{r}), & \mathbf{r} \in P_{m^+} \\ \dfrac{l_m}{2S_{m^-}}\vartheta_m^-(\mathbf{r}), & \mathbf{r} \in P_{m^-} \\ 0, & \text{elsewhere} \end{cases} \tag{2}$$

where l_m is the length of the nonboundary edge L_m, S_{m^+} and S_{m^-} are the areas of the triangular patches P_{m^+} and P_{m^-}, respectively, $\vartheta_m^+(\mathbf{r})$ and $\vartheta_m^-(\mathbf{r})$ are the vectors defined as shown in Figure 1(b), and $\mathbf{r}$ is the position vector of an arbitrary point on the conducting surface relative to the origin.

A matrix equation is formulated as

$$V_m = \sum_{n=1}^{N} Z_{mn} K_n, \quad m = 1, 2, \ldots, N \tag{3}$$

where V_m is excitation voltage difference applied across the mth nonboundary edge and Z_{mn} is the mutual impedance between the mth and nth nonboundary edges, which is evaluated as described in [5].

The linear system of equations described by (3) has N equations in N unknowns and can be solved for the unknown current distribution on the conducting surface.

2.1. The Conventional Method of Excitation Using Local Ports

The conventional method of attaching excitation voltage source to a conducting surface is described in [4] for a point-matching MoM and in [5] for a Galerkin's technique. In this section we generalize this method to attaching multiple sources to a conducting surface. A source port is a part of a conducting body over which an excitation voltage can be imposed. Let a number of source ports be defined on a conducting surface and let an integer x represent a source port index within all the defined source ports. The conventional method uses a nonboundary edge L_{m_x} as that shown in Figure 2 to represent the infinitesimal-width gap source, where m_x is the index of the specified nonboundary edge within all the nonboundary edges of the model. The current component normally crossing the edge L_{m_x} is equal to I_{m_x}, which is continuous across L_{m_x} and constant along it. The corresponding linear current density is, thus, $K_{m_x} = I_{m_x}/L_{m_x}$, which is also constant along L_{m_x}.

In some specific antenna feeding problems, the antenna has two separated arms or detached parts between which a voltage source

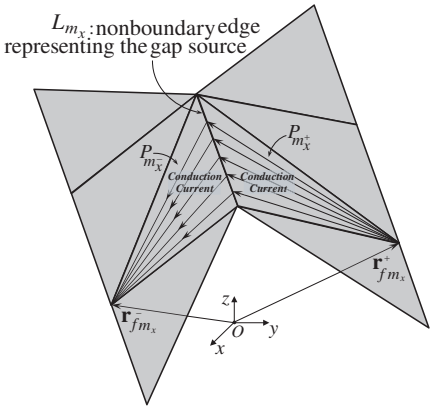

Figure 2. Conventional model for an infinitesimal gap source model.

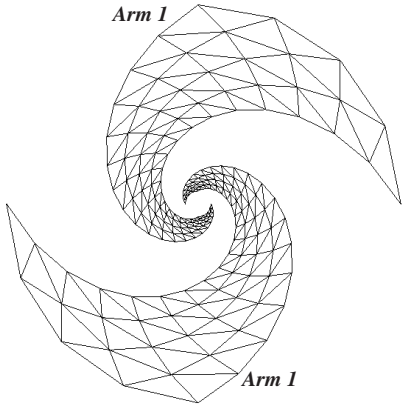

Figure 3. Triangular patch model for the planar spiral antenna.

should be applied, whereas the triangular-patch surface model for such an antenna does not possess a non-boundary edge to represent the excitation gap. An example for this case is the spiral antenna shown in Figure 3. In the conventional approach described above, to handle this case, an extra part, which is not a part of the actual antenna structure, must be added to the antenna model to attach the two separated parts or arms to enable the application of the exciting voltage across a gap represented by a non-boundary edge between the two antenna arms. The drawback of this conventional approach is that this part, which is artificially added to the antenna model just to enable the application of gap excitation, may be considered a modification of the antenna structure, which causes the surface model to be different from the actual antenna and thus affecting the accuracy of the obtained results. The artificially added part to the antenna model may contribute to the radiation and, hence, the (modified) antenna characteristics including the antenna impedance and radiation pattern may significantly differ from those of the actual antenna. An example for such a case is that shown in Figure 3 for a triangular patch model of a two-arm planar equiangular spiral antenna. A zoom-in view focused on the central part of the antenna is presented in Figure 4(a). As shown in the figure, the two arms are detached from each other. To apply a gap excitation to such an antenna, one may have to add a number of extra triangular patches to the antenna model to form a bowtie-like segment as that shown in Figure 4(b) in gray color. Adding this extra segment to the antenna model enables the application of an exciting voltage source across the infinitesimal gap represented by the central non-boundary edge which is shown as a thick line in Figure 4(b).

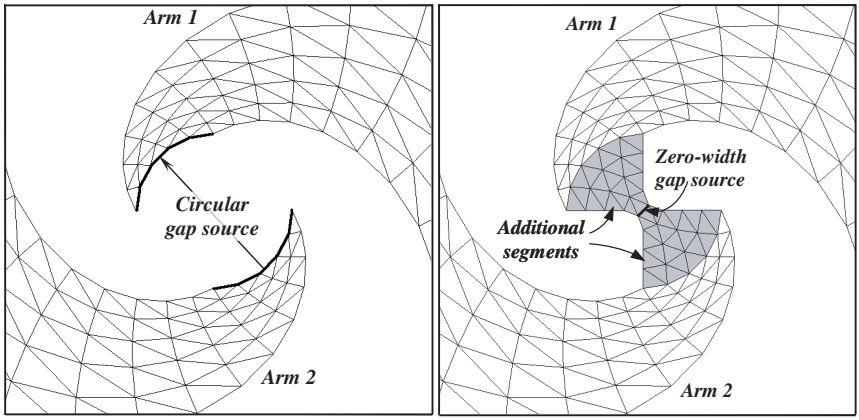

Figure 4. Zoom-in view at the central part of the spiral antenna showing (a) the circular arc edges between which an excitation voltage is required to be applied, and (b) an artificially added bowtie segment (the grayed triangles) to provide a central non-boundary edge across which an excitation voltage (gap source) can be applied.

2.2. The New Method of Excitation Using Realistic Local Port Model

In this paper, we introduce a new method to model the gap source. Instead of using a single non-boundary edge to represent the exciting gap, the proposed method uses a single or multiple pairs of facing boundary edges that form a real gap of arbitrary shape and width. This method has many advantages over the conventional (zero-width) gap source representation described above: Firstly, it does not require the addition of any extra segments to the antenna model. Secondly, unlike the conventional method that necessitates zero-width of the gap across which the exciting voltage difference is applied, the proposed method enables the representation of a gap source with arbitrary gap width. Thirdly, it enables the spatial variation of the applied excitation voltage (for the same source) along the length of the gap. Moreover, the proposed method enables the exciting gap to take arbitrary geometrical shape, which makes it a more appropriate model for exciting arbitrarily shaped structures.

A triangular-patch model for a conducting structure excited by a gap source of nonzero gap width is shown in Figure 5. The structure possesses 6 non-boundary edges and 12 boundary edges. Each non-boundary edge has unknown current crossing it normally. No current is allowed to cross a boundary edge unless it belongs to an excitation

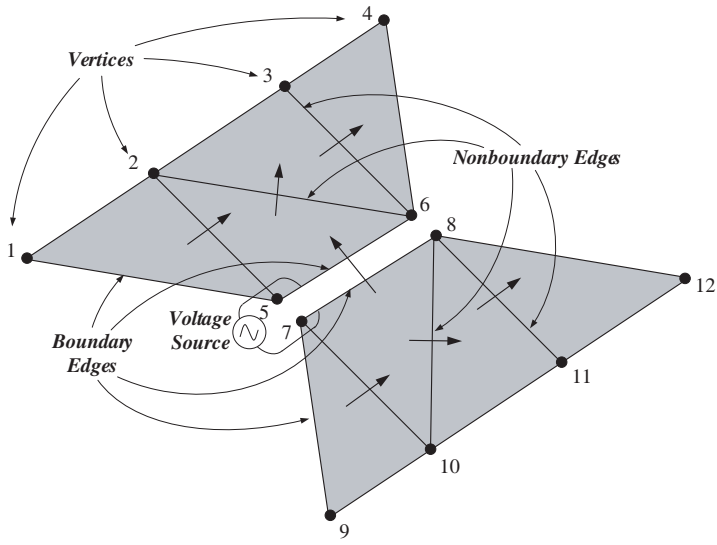

Figure 5. Triangular-patch model for a conducting surface excited by a gap of non-zero width. The surface model has 12 boundary edges, 6 non-boundary edges, and 7 current edges.

gap. The boundary edges constituting the excitation gap, shown in Figure 5, have current components passing normal to them through the excitation gap. This will be discussed in detail later on. In the EFIE formulation, this pair of boundary edges has unknown normal current component. Thus, the unknown currents to be determined using the MoM are those normally crossing the nonboundary edges as well as those passing through each pair of boundary edges constituting the excitation gaps. Considering the case shown in Figure 5, the structure has six non-boundary edges and one pair of boundary edges constituting the excitation gap. Hence, the total number of the unknown currents is 7. In the following discussions, all the edges (both boundary and nonboundary) that have normal current component will be referred to as *current edges*. According to this description, a current edge may be a single nonboundary edge or a pair of boundary edges constituting an excitation gap.

Instead of representing the gap source by a non-boundary edge across which a voltage difference is applied, the source gap is represented as a pair of boundary edges: $L^{+}_{m_{xi}}$ and $L^{-}_{m_{xi}}$ as shown in Figure 6, where m_{xi} is the global index of the specified boundary edges pair within all the current edges of the model, i is its index within the group of boundary edges pairs representing the specified source port and x is the index of the source port within all the source ports on the conducting surface model.

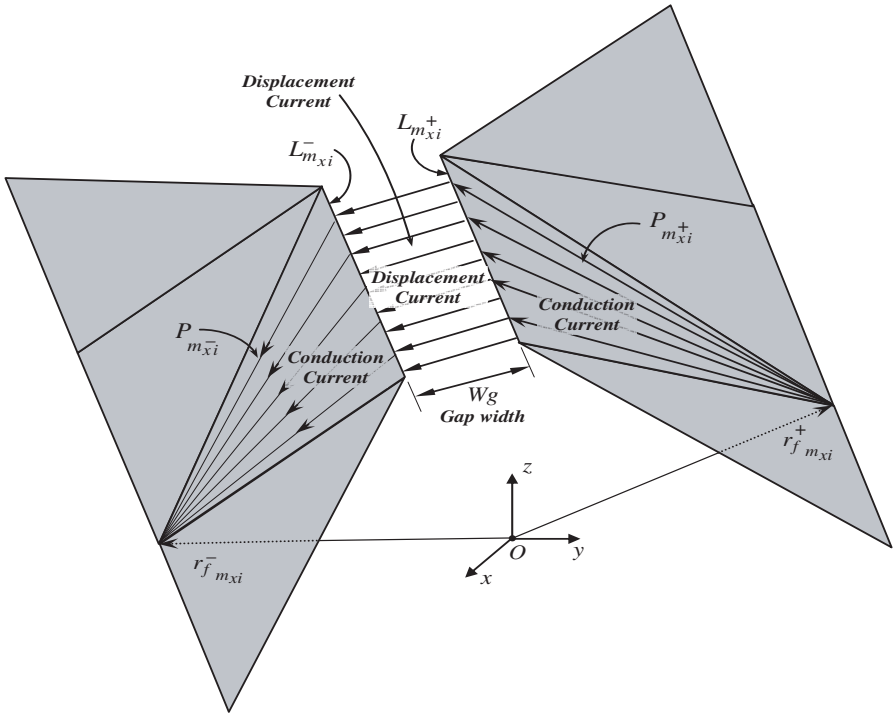

Figure 6. Proposed model for a gap source of non-zero width.

A displacement current $I_{m_{xi}}$ is assumed flowing across the gap where the positive reference direction is from the positive edge of the gap source $L^+_{m_{xi}}$ to the negative edge $L^-_{m_{xi}}$. The displacement field lines are normal to the gap edges at their start and end points. For source current continuity, the component of the current flowing out of $P_{m^+_{xi}}$ and normally crossing the edge $L^+_{m_{xi}}$ should be equal to the current component flowing into $P_{m^-_{xi}}$ and normally crossing the edge $L^-_{m_{xi}}$. Of course, this current component should be equal to $I_{m_{xi}}$.

According to the above description of the gap source representation, the unknown gap current $K_{m_{xi}}$ should be included in the unknown current vector $[I]$ of the MoM matrix equation and the gap voltage $V_{m_{xi}}$ should be included in the voltage vector $[V]$. This means that each gap source represented as a pair of facing boundary edges increases the dimensions of the Z matrix by adding a row: $Z_{m_{xi}n}; n = 1, 2, \ldots, N+1$ and a column: $Z_{mm_{xi}}; m = 1, 2, \ldots, N+1$ corresponding to $V_{m_{xi}}$ and $K_{m_{xi}}$, respectively. These additional impedance elements on their additional row and column of the matrix $[Z]$ should be evaluated.

3. NON-ZERO WIDTH GAP LOAD REPRESENTATION

A load port can be represented in the same way of representing a source port but with some differences. A load impedance is represented by a load gap which is modeled as a pair of boundary edges: $L^+_{m_{li}}$ and $L^-_{m_{li}}$, where m_{li} is the global index of the current edge within all the current edges of the model and i is its index within the group of boundary edges pairs representing the load port of index l within all the load ports in the model. The difference between the representation of a source and that of a load is that instead of including an additional gap voltage $V_{m_{xi}}$ in the voltage vector $[V]$ corresponding to each pair of boundary edges in a source port, a load impedance Z^L_{li} is added to the element of the matrix $[Z]$ that corresponds to each pair of boundary edges in the load port. This is described in detail as follows.

If a lumped load impedance $Z^L_{l_i}$ is attached to the conducting surface at the current edge number m_{l_i}, the connection is considered in series and, hence, it results in additional voltage drop equal to $Z^L_{l_i} I_{m_{l_i}}$ on crossing this current edge, which is added to the right hand side of (3) to get

$$V_{m_{l_i}} = Z^L_{l_i} I_{m_{l_i}} + \sum_{n=1}^{N} Z_{m_{l_i} n} I_n \tag{4}$$

This means that attaching a series lumped load impedance to a specific segment of the conducting surface is accounted for by adding the value of the load impedance to the original value of the self impedance of this segment in the matrix $[Z]$. Hence, one gets the modified self impedance expressed as

$$Z'_{m_{li} m_{li}} = Z_{m_{li} m_{li}} + Z^L_{li} \tag{5}$$

4. BASIS FUNCTION FOR THE GAP SOURCE AND THE GAP LOAD

Up to the author's knowledge, all the previous publications using the RWG basis functions require that the basis functions are defined only for the nonboundary edges, which means that each of the boundary edges has no current component crossing it. In the newly proposed method, the basis functions are not only defined for the nonboundary edges but also for each pair of boundary edges in a source or load gap. This requires the definition of a new basis function to describe the conduction current on the triangular patches $P_{m_x^+}$ and $P_{m_x^-}$ on the sides of the excitation gap, where m_x represents the index of the

specified pair of boundary edges within all the current edges. The following definition of the source/load basis function applies only when the pair $(L_{m_x}^+, L_{m_x}^-)$ belongs to a source port or a load port.

$$f_{m_x}(\mathbf{r}) = \begin{cases} \dfrac{l_{m_x}^+}{2S_{m_x^+}} \vartheta_{m_x}^+(\mathbf{r}), & \mathbf{r} \in P_{m_x^+} \\ \dfrac{l_{m_x}^+}{2S_{m_x^-}} \vartheta_{m_x}^-(\mathbf{r}), & \mathbf{r} \in P_{m_x^-} \end{cases} \tag{6}$$

It should be noted from the definition of f_{m_x} given by (6), that unlike the basis functions defined for the nonboundary edges, the component of f_{m_x} normal to the boundary edges of the excitation gap suffers a discontinuity when crossing the gap from $P_{m_x^+}$ to $P_{m_x^-}$. Furthermore, the linear current density crossing the edge $L_{m_x}^+$ is $K_{m_x}^+ = I_{m_x}/l_{m_x}^+$ at all the points on $L_{m_x}^+$, whereas the linear current density crossing the edge $L_{m_x}^-$ is $K_{m_x}^- = I_{m_x}/l_{m_x}^-$at all the points on $L_{m_x}^-$. Thus the linear current densities crossing $L_{m_x}^+$ and $L_{m_x}^-$ are not the same. Nevertheless, this has no concern with the current continuity across the gap source as the current components normal to $L_{m_x}^+$ and $L_{m_x}^-$ are equal. Hence, the current flowing into the gap source is equal to the current flowing out of it.

Let us define

$$G\left(\mathbf{r}, \mathbf{r}'\right) = \frac{e^{-jk_o|\mathbf{r}-\mathbf{r}'|}}{|\mathbf{r}-\mathbf{r}'|}, \tag{7}$$

and

$$G_{cp}\left(\mathbf{r}'\right) = G\left(\mathbf{r}_{cp}, \mathbf{r}'\right) \tag{8}$$

where $\mathbf{r}_{cp}$ is the centroid of the triangular patch P_p.

By following the procedure applied in [3] and making the necessary modifications according to the new consideration of the source and load representation, we arrive at the following expressions for the elements of the Z matrix.

$$Z_{mn} = j\omega\, \alpha_{mn} + \beta_{mn} \tag{9}$$

where,

$$\alpha_{mn} = \alpha_{mn}^{m^+n^+} + \alpha_{mn}^{m^+n^-} + \alpha_{mn}^{m^-n^+} + \alpha_{mn}^{m^-n^-} \tag{10}$$

$$\beta_{mn} = \beta_{mn}^{m^+n^+} + \beta_{mn}^{m^+n^-} + \beta_{mn}^{m^-n^+} + \beta_{mn}^{m^-n^-} \tag{11}$$

$$\alpha_{mn}^{m^+n^+} = \frac{\mu_o}{16\pi} \frac{1}{S_{n^+}} \vartheta_{c_m}^+ \cdot \left(\int_{P_{n^+}} \vartheta_n^+ G_{cm^+} dS' \right) \tag{12}$$

$$\alpha_{mn}^{m^+n^-} = \frac{\mu_o}{16\pi}\frac{1}{S_{n^-}}\vartheta_{c_m}^{+}\cdot\left(\int\limits_{P_{n^-}}\vartheta_n^{-}G_{cm^+}dS'\right) \tag{13}$$

$$\alpha_{mn}^{m^-n^+} = \frac{\mu_o}{16\pi}\frac{1}{S_{n^+}}\vartheta_{c_m}^{-}\cdot\left(\int\limits_{P_{n^+}}\vartheta_n^{+}G_{cm^-}dS'\right) \tag{14}$$

$$\alpha_{mn}^{m^-n^-} = \frac{\mu_o}{16\pi}\frac{1}{S_{n^-}}\vartheta_{c_m}^{-}\cdot\left(\int\limits_{P_{n^-}}\vartheta_n^{-}G_{cm^-}dS'\right) \tag{15}$$

$$\beta_{mn}^{m^+n^+} = \frac{1}{j\omega 4\pi\varepsilon_o S_{n^+}}\int\limits_{P_{n^+}}G_{cm^+}dS' \tag{16}$$

$$\beta_{mn}^{m^+n^-} = \frac{-1}{j\omega 4\pi\varepsilon_o S_{n^-}}\int\limits_{P_{n^-}}G_{cm^+}dS' \tag{17}$$

$$\beta_{mn}^{m^-n^+} = \frac{-1}{j\omega 4\pi\varepsilon_o S_{n^+}}\int\limits_{P_{n^+}}G_{cm^-}dS' \tag{18}$$

$$\beta_{mn}^{m^-n^-} = \frac{1}{j\omega 4\pi\varepsilon_o S_{n^-}}\int\limits_{P_{n^-}}G_{cm^-}dS' \tag{19}$$

5. DISTRIBUTED GAP SOURCES OF ARBITRARY SHAPE

For a wide strip dipole antenna as that shown in Figure 7, the gap made to apply a voltage source excitation should have its length equal to the width of the strip dipole. Such a wide dipole should be divided along its width into many segments for accurate computation of the current distribution on the antenna surface and which allows the accurate computation of the antenna input impedance and the near field and far field quantities. Thus, each of the gap edges has multiple segments (boundary edges) each of which is a boundary edge in the triangular patch model of the strip dipole. A voltage difference is applied between the boundary edges of each of the pairs: (L_{m11}^{+}, L_{m11}^{-}), (L_{m12}^{+}, L_{m12}^{-}), and (L_{m13}^{+}, L_{m13}^{-}) as shown in Figure 7. If the excitation voltage is assumed to be uniform over the edge length (i.e., the strip width) then the applied voltage for each pair of the boundary edges forming the gap should be the same. The gap excitation can be seen as parallel

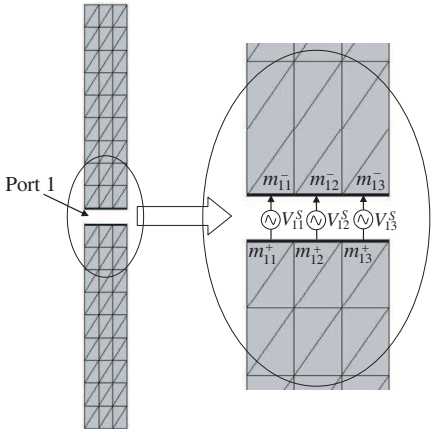

Figure 7. Gap voltage excitation for a widestrip dipole antenna.

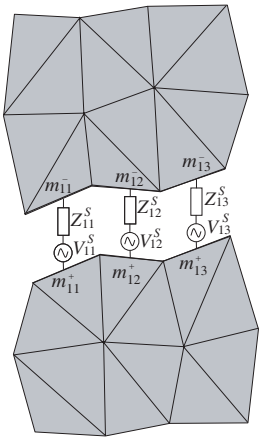

Figure 8. Arbitrarily shaped distributed gap-source with distributed internal impedance.

combination of the voltage sources applied between the edges of each pair of the boundary edges.

5.1. Calculating the Input Impedance of a Conducting Surface Excited by Distributed Gap Source

The input impedance of the wide-strip dipole antenna evaluated using an arbitrarily-shaped distributed gap source model is obtained by calculating the parallel combination of Z_{11}^{in}, Z_{12}^{in}, and Z_{13}^{in}, where

$$Z_{11}^{\text{in}} = \frac{V_{m_{11}}}{I_{m_{11}}}, \quad Z_{12}^{\text{in}} = \frac{V_{m_{12}}}{I_{m_{12}}}, \quad Z_{13}^{\text{in}} = \frac{V_{m_{13}}}{I_{m_{13}}} \tag{20}$$

where $I_{m_{11}}$, $I_{m_{12}}$, and $I_{m_{13}}$ are the surface currents flowing out of the triangular patches $P_{m_{11}^+}$, $P_{m_{12}^+}$, and $P_{m_{13}^+}$, respectively, and normally crossing the boundary edges $L_{m_{11}}^+$, $L_{m_{12}}^+$, and $L_{m_{13}}^+$, respectively. These currents can be obtained using the well known procedure of the MoM. To calculate the input impedance one should calculate Z_{11}^{in}, Z_{12}^{in}, and Z_{13}^{in} using (9) and then the input impedance is calculated as follows.

$$\frac{1}{Z^{\text{in}}} = \frac{1}{Z_{11}^{\text{in}}} + \frac{1}{Z_{12}^{\text{in}}} + \frac{1}{Z_{13}^{\text{in}}} \tag{21}$$

Also, if we refer to Figure 7, we can substitute for voltage vector elements appearing in (20) as:

$$V_{m_{11}} = V_{11}^S \tag{22a}$$

$$V_{m_{12}} = V_{12}^S \tag{22b}$$
$$V_{m_{13}} = V_{13}^S \tag{22c}$$

5.2. Arbitrarily-Shaped Distributed Gap Source with Internal Impedance

The proposed method enables the excitation gap to have arbitrary geometry as shown in Figure 8. The exciting voltages can be distributed along the gap as shown in the same figure. The applied voltage sources can have internal impedances as those shown in Figure 8. In this case, the Z-matrix should be modified by adding the internal impedances to the original values of the corresponding Z-matrix elements as follows:

$$Z'_{m_{11}m_{11}} = Z_{m_{11}\,m_{11}} + Z_{11}^S \tag{23a}$$
$$Z'_{m_{12}m_{12}} = Z_{m_{12}\,m_{12}} + Z_{12}^S \tag{23b}$$
$$Z'_{m_{13}m_{13}} = Z_{m_{13}\,m_{13}} + Z_{13}^S \tag{23c}$$

6. RESULTS AND DISCUSSIONS

In the following discussions, we present some numerical results to examine the dependence of the antenna input impedance on the excitation gap width, the effect of the geometrical shape of the excitation gap on the antenna input impedance. Also, we study the dependence of the antenna input impedance on the resolution or segmentation along the gap length.

6.1. Effect of the Excitation Gap Width on the Antenna Input Impedance

The capability of the modeling a gap source of nonzero width in the MoM solution using the method described in Section 2 enables the study of the dependence of the antenna input impedance on the excitation gap width. An example is a straight strip dipole antenna of 7.255 cm length and 1.81 mm width operating at 2 GHz. The geometrical model of the strip dipole is shown in Figure 9. The dipole has two arms each of which is divided into seven rectangular segments along its length and one segment along its width. Each rectangular segment is divided into two triangular patches. The dependence of the input impedance on the gap width is investigated in two cases. In the first case, the total dipole length L_d, is kept constant while increasing the gap width W_g. This means that arm length L_a varies with varying the gap width, i.e., $L_a = (L_d - W_g)/2$. In the other case,

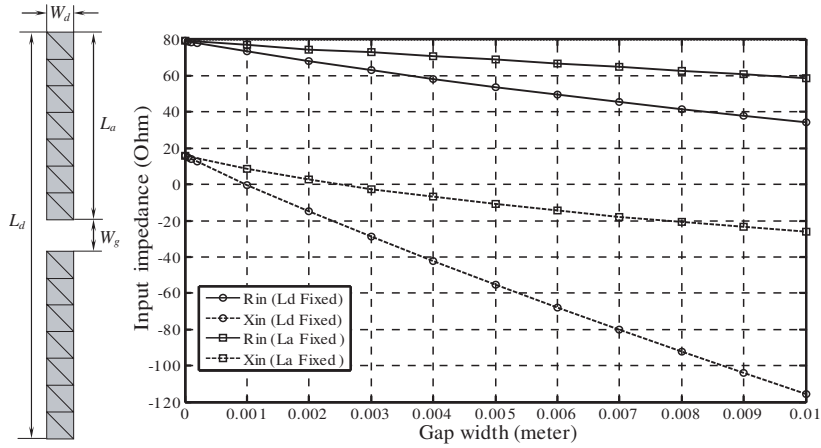

Figure 9. Dependence of a straight strip dipole antenna impedance on the gap width of the exciting gap source. The strip dipole has a length of 7.255 cm and a width of 1.81 mm. The operating frequency is 2 GHz.

the arm length is kept constant while varying the gap width, which means that the total dipole length increases with increasing the gap width, i.e., $L_d = 2L_a + W_g$. In both cases, the resistive and the reactive parts of the input impedance decrease with increasing the gap width as shown in Figure 9. The reactive part shows stronger dependence on the gap width as it decreases much more rapidly than the resistive part. The second case, in which the arm length is kept of constant length while the total dipole length increases with increasing the gap width, shows less dependence on the gap width. This means that the input impedance of the strip dipole antenna is much more dependent on the length of the conducting arms rather than the gap width. However, the latter has a significant effect on the antenna impedance, especially its reactive part. With increasing the gap width, the strip dipole antenna impedance becomes more capacitive.

6.2. Current Distribution along the Excitation Gap Length

One of the major advantages of the proposed technique is its ability of studing the current distribution along the edges of the gap. The conventional technique uses only one (non-boundary) edge for the gap source representation, which does not allow the variation of the current along the gap. The newly proposed method allows the voltage source to be represented by multiple (adjacent) edges along the gap and, thereby,

enables the current distribution to be correctly distributed along the gap length. This becomes more essintial in the cases of long excitation gap.

The following four figures show the current distribution along the excitation gap length for a strip dipole excited by a gap source of 1 mm width. In these four cases, the gap length varies as: 20 mm for the results presented in Figure 10, 7.255 mm for Figure 11, 3.6275 mm for Figure 12 and, finally, 1.451 mm for Figure 13. In all these cases, the number of segments taken along the gap length is 6. The objective of such a presentation is to show the necessity of using multiple segments along the gap length especially for long gaps.

Figure 10 shows the variation of the input current to a strip dipole antenna along the gap length in the case of a long gap (20 mm). The current has singular behavior at the ends of the gap edge, which is known as the edge behavior. Except for the two ends of the excitation gap, the current seems to be constant along the gap length. This is not the same behavior in the case of a narrow strip dipole (1.451 mm) for which the current distribution is presented in Figure 13 in spite of dividing the gap length to the same number of segments. The current distribution over the gap length seems to require a less number of segments along the narrow gaps.

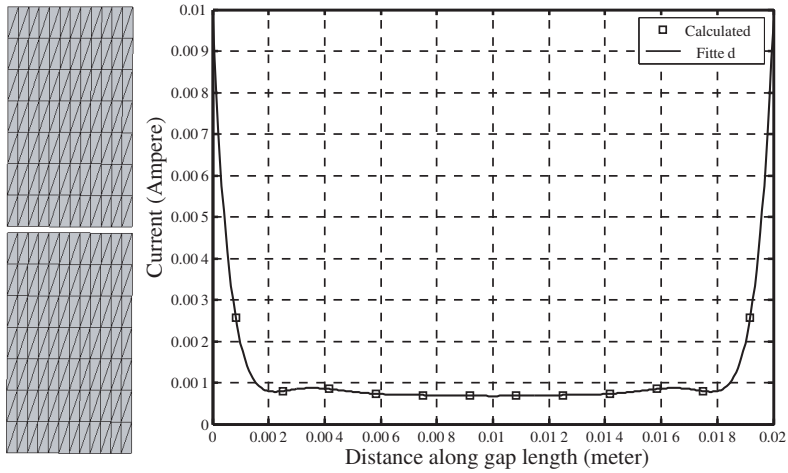

Figure 10. Current distribution (magnitude) along the excitation gap length. Dipole length = 7.255 cm, width = 2 cm, gap width 1 mm, number of segments along one arm = 7, number of segments along the strip width = 12, and $f = 2$ GHz.

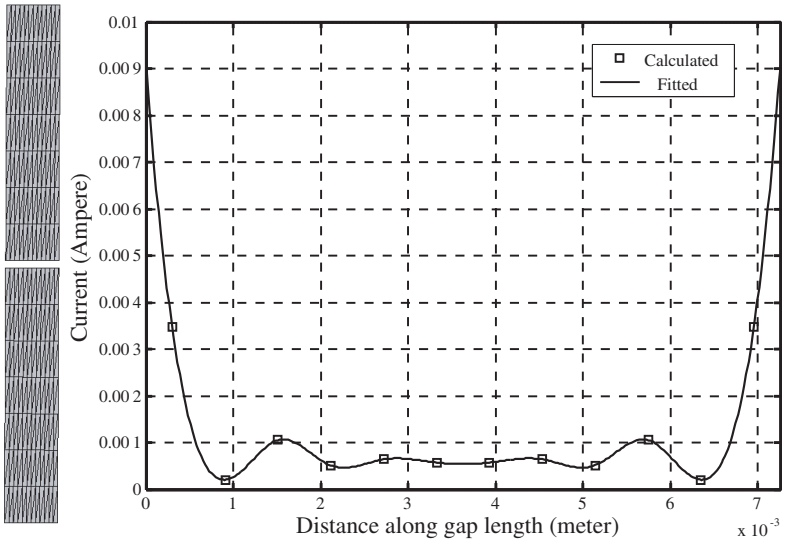

Figure 11. Current distribution (magnitude) along the excitation gap length. Dipole length = 7.255 cm, width = 0.7255 cm, gap width 1 mm, number of segments along one arm = 7, number of segments along the strip width = 12, and $f = 2$ GHz.

6.3. Dependence of the Antenna Input Impedance on the Geometrical Shape of the Excitation Gap

The method proposed in Section 2 to model a gap source of arbitrary shape is applied here to construct a gap source excitation of a planar spiral antenna whose geometrical model is shown in Figure 3. Recall that, as described in Section 2, the conventional gap source excitation of such an antenna requires the addition of extra triangular segments to the geometrical model of the spiral antenna to enable the application of a voltage source across the gap represented by the central boundary edge as shown in Figure 4(b). The newly proposed method enables us to model a circular gap with multiple boundary edges and distributed voltage excitation. The circular gap model is shown in Figure 14(a) where some extra triangular segments, shown in gray color in Figure 14, are added to enable the variation of the circular gap diameter. A straight gap of non-zero width can also be used to excite this antenna as shown in Figure 14(b).

It may be worth to mention that, in the case of a circular exciting gap with a diameter equal to the inner diameter of the spiral antenna as shown in Figure 4(a), no additional segments are required. In this case, a distributed voltage source can be applied as shown in Figure 15.

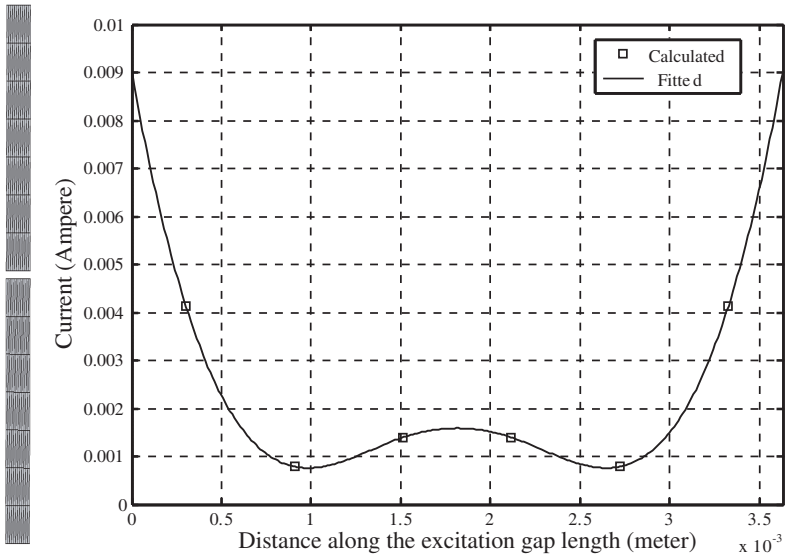

Figure 12. Current distribution (magnitude) along the excitation gap length. Dipole length = 7.255 cm, length = 0.36275 cm, gap width 1 mm, number of segments along one arm=11, number of segments along the strip width = 6, and f = 2 GHz. Input impedance = $79.04 + j5.68$.

In the following discussion, a comparison is made between the value of the antenna input impedance obtained when a circular gap source is used and that obtained when a straight gap source is used. The variation of the input impedance of such an antenna with varying the diameter of the circular gap model as well as the width of the straight gap model is presented in Figure 16. As shown in Figure 16(a), no significant difference between the values of the resistive parts of the input impedance obtained using the two models. On the other hand, the values of the reactive parts shows significant dependence on the geometrical model of the gap source as shown in Figure 16(b). As the diameter of the circular gap and the width of the straight gap approach the inner diameter of the spiral, the values of the reactive part of the input impedance obtained using the two models approach each other.

6.4. Dependence of the Antenna Input Impedance on the Segmentation along the Gap Length

In this section, the effect of the number of segments taken along the gap length on the calculated value of the antenna input impedance

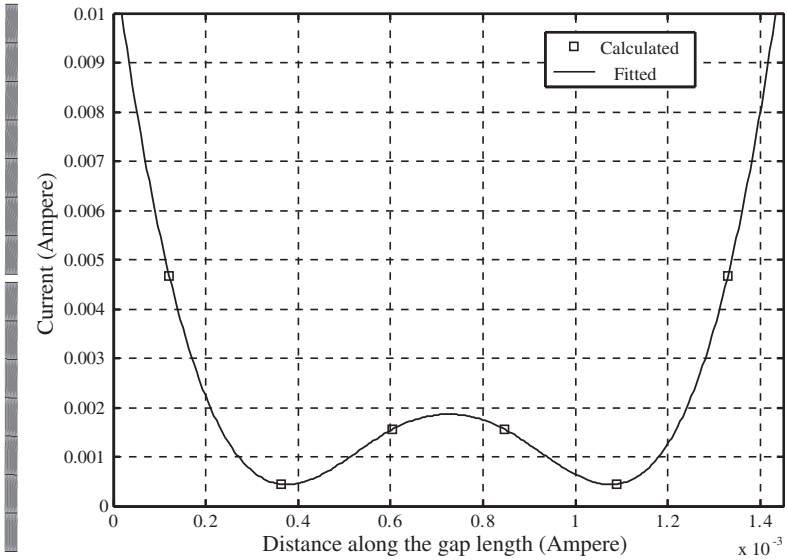

Figure 13. Current distribution (magnitude) along the excitation gap length. Dipole length = 7.255 cm, width = 0.1451 cm, gap width 1 mm, number of segments along one arm = 21, number of segments along the strip width = 6, and $f = 2$ GHz. Input impedance = $74.77 + j2.87$.

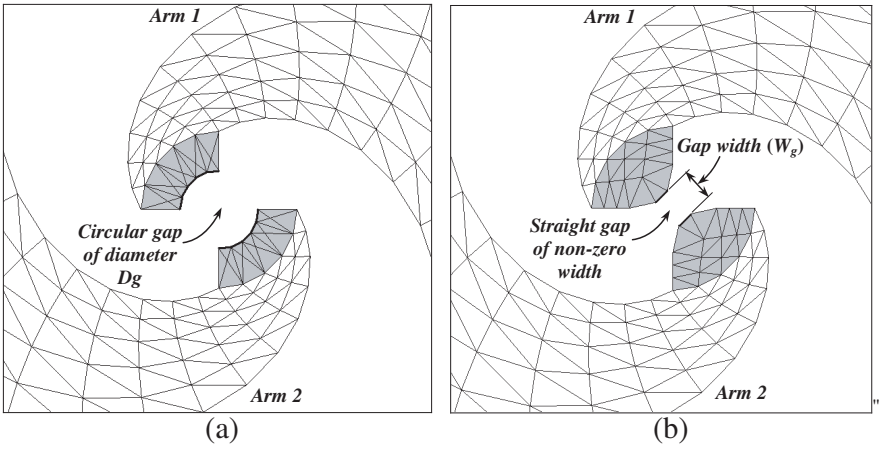

Figure 14. Triangular patch model for the spiral antenna excited by (a) a circular gap source, and (b) a straight gap source.

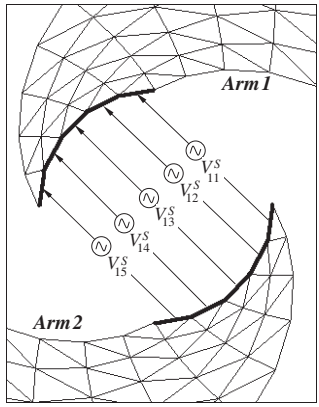

Figure 15. Application of distributed voltage excitation between the facing segments of the circular edges constituting the inner circle of a two-arm spiral antenna.

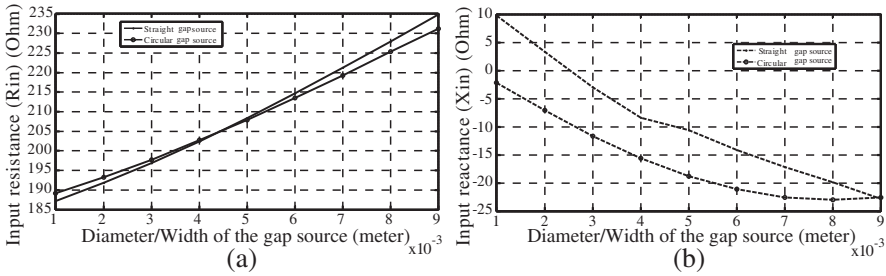

Figure 16. Variation of (a) the resistive part and (b) the reactive part of the input impedance of a planar spiral antenna with changing the gap width or diameter when using a straight gap model and a circular gap model of the source. The spiral inner diameter = 1 cm, end angle = 1.5π (270°), arm width = 90°, winding angle = 60°, and $f = 2$ GHz.

is investigated.

As shown in Figure 17, the calculated value of the input impedance of a strip dipole approaches its exact value with increasing the number of segments taken along the gap length (strip width). However, good accuracy of the calculated antenna impedance (about 5% error) is obtained even when a single segment is taken along the gap length.

As shown in Figure 18, the calculated value of the input impedance of a wide strip dipole approaches its exact value with increasing the number of segments taken along the gap length (strip width). However,

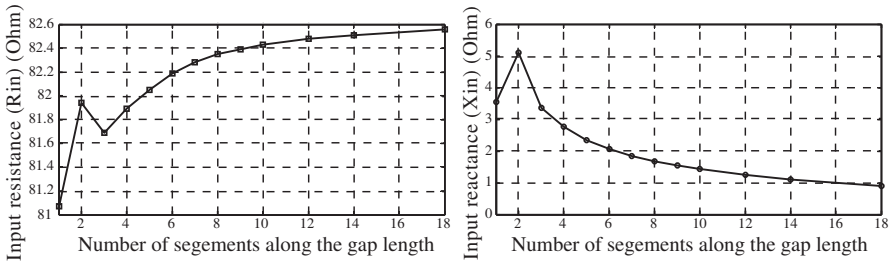

Figure 17. Dependence of the calculated value of the input impedance of a straight strip dipole antenna on the resolution of segmentation of the excitation gap edges. Dipole length = 7.255 cm, width = 0.7255 cm, gap width 1 mm, number of segments along one arm = 7, and $f = 2$ GHz.

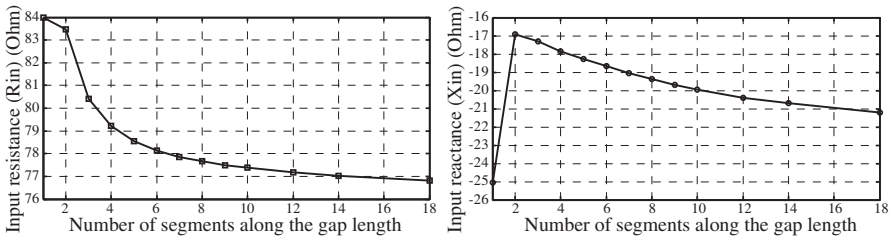

Figure 18. Dependence of the calculated value of the input impedance of a wide straight strip dipole antenna on the resolution of segmentation of the excitation gap edges. Dipole length = 7.255 cm, width = 2 cm, gap width 1 mm, number of segments along one arm = 7, and $f = 2$ GHz.

an error of about 9% of the calculated antenna impedance is obtained when a single segment is taken along the gap length compared to the value of the input impedance calculated when 18 segments are taken along the gap length. Comparing the results presented in Figure 17 to those presented in Figure 18 for a wider strip dipole, it becomes clear that the accuracy of the calculated antenna impedance requires finer segmentation as the excitation edge length becomes wider.

7. CONCLUSION

A method is described to model the excitation and loading for antennas composed of arbitrarily shaped conducting surfaces. Instead of using a single non-boundary edge to represent a zero-width exciting gap

according to the conventional method, the proposed method uses either single or multiple pairs of facing boundary edges to form a real gap of arbitrary shape and width. It is shown that the new method has many advantages over the conventional (zero-width) source/load representation. The proposed method provides more flexibility in shaping the gap to fit the antenna surface. Also, the results obtained for the antenna input impedance and the input current distribution are much more accurate. Numerical results are obtained to investigate the dependence of the antenna input impedance and the current distribution along the gap length on the gap width, the geometrical shape of the gap and the surface segmentation resolution along the gap length. It is shown that using multiple segments along the excitation gap is necessary to get the correct current distribution especially for long gaps.

REFERENCES

1. Gibson, W. C., "The method of moments in electromagnetic," Chapman & Hall/CRC, New York, London, 2008.
2. Chen, Q., Q. Yuan, and K. Sawaya, "Accurate source model for MoM analysis of linear antennas by using sinusoidal reaction matching technique," *IEICE Trans. Commun.*, Vol. E86-B, No. 2, Feb. 2003.
3. Rao, S. M., D. R. Wilton, and A. W. Glisson, "Electromagnetic scattering by surfaces of arbitrary shape," *IEEE Trans. Antennas Propagat.*, Vol. 30, 409–418, May 1982.
4. Makarov, S. N., *Antenna and EM Modeling with Matlab*, John Wiley, New York, 2002.
5. Hussein, K. F. A., "Accurate computational algorithm for calculation of input impedance of antennas of arbitrarily shaped conducting surfaces," *Applied Computational Electromagnetics Society, ACES Journal*, Vol. 22, No. 3, Nov. 2007.
6. Maaskant, R. and M. Arts, "Reconsidering the voltage-gap source model used in moment methods," *IEEE Antennas and Propagation Magazine*, Vol. 52, No. 2, 120–125, Apr. 2010.
7. Lo, Y. H., S. Q. He, L. J. Jiang, and W. C. Chew; "Finite-width gap excitation and impedance models," *IEEE International Symposium on Antennas and Propagation (APSURSI)*, 1297–1300, 2011.